Resonant and off-resonant phenomena in double-barrier interband tunneling structures

A. Nogaret,* M. A. Maldonado, R. E. Carnahan, K. P. Martin, and R. J. Higgins
School of Electrical Engineering and Microelectronics Research Center, Georgia Institute of Technology, Atlanta, Georgia 30332

F. Aristone, D. K. Maude, and J. C. Portal
Laboratoire de Physique des Solides, Institut National des Sciences Appliquées, 31077 Toulouse CEDEX, France and Service National des Champs Intenses, Centre National de la Recherche Scientifique, 38042 Grenoble CEDEX, France

J. F. Chen† and A. Y. Cho
AT&T Bell Laboratories, Murray Hill, New Jersey 07974

(Received 8 September 1992; revised manuscript received 28 December 1992)

We report the results of vertical-transport measurements performed on a GaSb/AlSb/InAs/AlSb/InAs interband tunneling structure subjected to hydrostatic pressure and high magnetic fields applied both parallel and perpendicular to the current. Current-voltage characteristics exhibit both a main peak and a weaker feature at lower bias voltages whose behavior is compared to that of the main peak. Our analysis reveals that the effective current in the device can be viewed as the sum of an Esaki diodelike current and a resonant current associated with the ground state in the InAs well.

Tunneling studies in type-II semiconductor heterostructures composed of InAs, AlSb, and GaSb have recently been initiated because these systems present an alternative to type-I resonant tunneling. Electrons and holes are spatially separated at an InAs/GaSb heterojunction, with the InAs conduction-band (CB) edge lying below the GaSb valence-band (VB) edge by an amount $\Delta=0.15$ eV (under flat-band conditions).[1] Within that energy width, InAs CB states can couple to GaSb VB states. Thus vertical transport involves conduction of both electrons and holes known as interband tunneling. Wide-band-gap (2.3-eV) (Ref. 2) AlSb layers are used to define potential barriers. Proper juxtapositions of these different material layers offer the opportunity for designing new devices that combine the electronic properties of the Esaki diode with those of the resonant-tunneling diode. On the one hand, interband tunneling between InAs and GaSb permits, at room temperature, tunnel diodelike characteristics with moderate peak-to-valley ratios and small excess currents.[3] On the other hand, AlSb layers can be inserted in order to confine electrons (or holes) close to the InAs/GaSb interface. It was shown (Refs. 4–7) that peak current densities are enhanced by the creation of resonant levels. These affect the conductance, since electrons tunneling resonantly must now satisfy conditions of energy and momentum conservation. In type-II tunneling, in-plane momentum conservation rules the resonance onset voltage,[8] whereas the resonance cutoff is determined by energy conservation conversely to type-I tunneling. This also implies a reduced scattering contribution to the valley current. In fact, peak-to-valley ratios as high as 20:1 (80:1) at 300 K (77 K) have been observed in interband tunneling devices.[6,7]

This work investigates an InAs quantum-well, AlSb double-barrier structure with one InAs electrode and one GaSb electrode, such that a mixture of both interband and type-I resonant tunneling is expected to occur. The structure was grown by molecular-beam epitaxy (MBE) on a (100)-oriented p^+-type GaSb substrate and successively composed of (i) a $p^+=5\times10^{18}$ cm^{-3} Be-doped GaSb buffer, (ii) a 5-nm undoped GaSb spacer layer, (iii) a 1.5-nm undoped AlSb barrier, (iv) a 16-nm undoped InAs well, (v) a 1.5-nm undoped AlSb barrier, (vi) a 5-nm undoped InAs spacer layer, and (vii) a $n^+=1\times10^{18}$ cm^{-3} Si-doped InAs buffer. Mesas were defined by wet chemical etching and top Ohmic contacts were nonalloyed.

The potential profile throughout the structure, calculated with a Poisson solver, can be seen in Fig. 1. Free charges present in the active region of the device at equilibrium lead to strong deviations from flat-band conditions (the inset of Fig. 1). Taking into account the non-

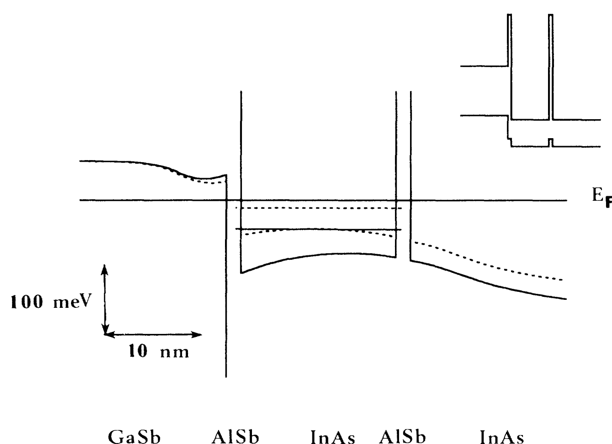

FIG. 1. Band profiles at P=ambient (full line) and $P=10$ kbar (dashed line) for the double-barrier interband tunnel structure at thermal equilibrium. The Fermi energies and the positions of the bound levels in the well are also given. The flat-band potential profile of the heterostructure is given in the inset.

 ©1993 The American Physical Society

parabolicity of the InAs CB, the energies of the quasi-bound levels in the well have been derived from the transmission spectrum of the equivalent InAs quantum-well, AlSb double-barrier structure, with InAs used for both electrodes. The ground and first excited states are, respectively, 36 and 159 meV above the CB edge in the center of the well. The first excited state is always aligned with evanescent states in the GaSb band gap, and only the ground state is resonant. No other bound levels are available to affect the transmissivity in the range of bias voltages considered in this work. In particular, the narrowness of the GaSb spacer layer precludes the formation of hole levels in this accumulation region. Hence the hole distribution in the vicinity of the barrier is purely three dimensional.

Current-voltage (I-V) measurements performed on all samples show a shift of their characteristics to higher bias voltage (V_b) when cooling to lower temperatures (the inset of Fig. 2). This change is not due to an intrinsic property of the heterostructure since the current remains constant. Thus we ascribe this voltage shift to a $R_c^{\Delta T}=10$ Ω increase in the Ohmic resistance of the contacts that is consistent with further quantitative examination. As a consequence of sample asymmetry, the I-V curve strongly differs depending on the bias polarity. Reverse bias (substrate negative) characteristics (not shown here) exhibit behavior similar to a reverse-biased Esaki diode[9] that here is the macroscopic expression of the potential experienced by the electrons tunneling in the AlSb barriers. At 4.2 K, forward bias (substrate positive) traces exhibit a nearly triangular peak at $V_b=V_p=310$ mV, with a broad feature at $V_b=V_f=92$ mV in the region of increasing current (Fig. 2). The weakness of the peak-to-valley ratio, 4.2:1 (2.6:1) at 4.2 K (300 K), is essentially due to a strong valley current. This effect is known to be related to high concentrations of extrinsic defect states introduced into the band gap because of high donor and acceptor doping levels in the contacts.[10]

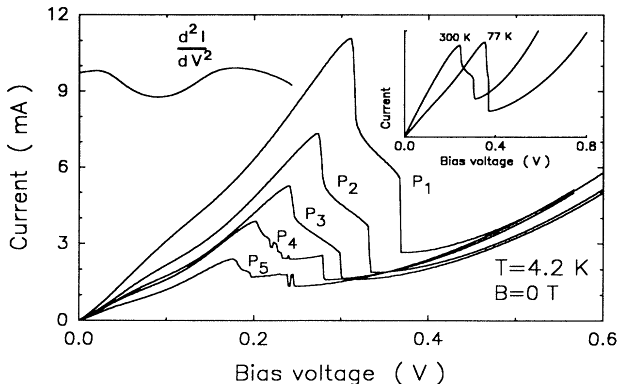

FIG. 2. Forward bias current-voltage characteristics at different hydrostatic pressures and zero magnetic field for the sample described in the text. ($P_1=1.35$ kbar, $P_2=3.57$ kbar, $P_3=5.67$ kbar, $P_4=7.59$ kbar, $P_5=10.13$ kbar.) The inset shows the characteristic of the same sample at 300 and 77 K at ambient pressure. The voltage position of the feature (V_f) is found at the minimum of the second derivative of the current (plotted here for $P=1.35$ kbar).

The I-V characteristic can be qualitatively understood independently of a consideration of the transmission probability by simply counting the number of active conducting channels allowed when the electron and hole distributions overlap. By a conducting channel we mean a CB state and a corresponding *empty* VB state with the same energy and in-plane momentum, so that charges can transfer coherently from one to another. Moreover, a conducting channel is said to be active if its CB state is populated. With this picture, we distinguish two current components: (i) a resonant current consisting of electrons tunneling resonantly through the two-dimensional (2D) bound states in the InAs well, and (ii) an off-resonant current involving all other electrons from the 3D distribution in the InAs electrode that occupy states with evanescent decaying probabilities in both the barriers and the well. Resonant and off-resonant tunneling paths coexist as two parallel processes, so that the total current is simply the sum of a resonant current and an Esaki diodelike current. To clarify this idea, we point out that the resonant current component can be suppressed by making the well width tend to zero. This hypothetical system is then analogous to an Esaki diode. In the following, we define $N_{2\mathrm{D}}(V_b)$ and $N_{3\mathrm{D}}(V_b)$ as the number of active conducting channels at bias voltage V_b whose CB states are occupied by electrons from the 2D and 3D distribution, respectively. $N_{2\mathrm{D}}(V_b)$ and $N_{3\mathrm{D}}(V_b)$ have been calculated for our structure and plotted in Fig. 3(b). Within the assumption of a Lorentzian broadening of the resonant level, the resonant current can be expressed by

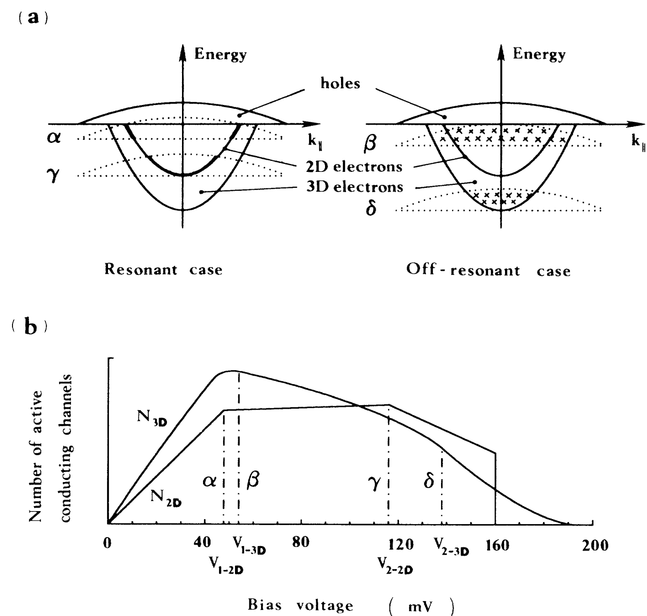

FIG. 3. The schematic correspondence between the band alignments (a) and the turning points observed in the plot of the number of active conducting channels (b) allowed when the current is resonant $N_{2\mathrm{D}}(V_b)$ and off-resonant $N_{3\mathrm{D}}(V_b)$. The crossed area (bold lines) is a diagrammatic representation of $N_{3\mathrm{D}}(V_b)$ $[N_{2\mathrm{D}}(V_b)]$. The cutoff of $N_{2\mathrm{D}}(V_b)$ is due to in-plane momentum conservation as in type-I resonant tunneling.

$$I=eN_{2D}(V_b)\frac{\Gamma}{\hbar}T_{res} , \quad (1)$$

where Γ is the resonant-level energy half-width, T_{res} the transmission probability at resonance, and e the charge of a single electron. The off-resonant current was calculated by Kane,[11] and presents the same global behavior as $N_{3D}(V_b)$. It is convenient to visualize the main stages of the electron and hole distributions overlapping in an energy versus in-plane momentum diagram [Fig. 3(a)] and relate them to the turning points seen in $N_{2D}(V_b)$ and $N_{3D}(V_b)$ [Fig. 3(b)] and those seen in the I-V's.

As soon as a forward bias is applied, electrons in the InAs emitter with energies in the range of eV_b below the electron quasi-Fermi level may tunnel into available GaSb valence states [$\varepsilon_{Fe,3D}=138$ meV ($\varepsilon_{Fh}=54$ meV) is the Fermi energy for 3D electrons (holes)]. The resonant current begins immediately upon application of bias because the Fermi wave vector for holes ($k_{Fh}\simeq 0.67$ nm^{-1}) is larger than that of the two-dimensional electron distribution in the well ($k_{Fe,2D}<k_{Fe,3D}$;$k_{Fe,3D}\simeq 0.31$ nm^{-1}) [Fig. 3(a)]. In-plane momentum conservation can always be realized,[8] thus active conducting channels involving 2D electrons and 3D holes exist at vanishingly small biases. Similarly, active conducting channels involving 3D electrons and 3D holes are formed as soon as the hole distribution overlaps in energy the 3D electron distribution; therefore the off-resonant current also starts increasing from zero bias.

First, a qualitative discussion of both the lower bias feature at $V_b=V_f$ and the peak at $V_b=V_p$ will be given. The low bias feature occurs when the voltage-induced overlap of the hole distribution by the electron distribution (either 2D or 3D) becomes such that all the conducting channels in the system are activated. At this point, further increase in bias leads to a kink in the current because no more conducting channels can be added through the hole distribution. The onset of this saturation occurs at two different biases for the resonant [Fig. 3(a) case α] and off-resonant [Fig. 3(a), case β] currents. In the first case, the resonant current rate of increase abruptly falls to a lower value when the applied voltage exceeds

$$eV_{1\text{-}2D}=\frac{\hbar^2}{2m_h^*}(k_{Fh}^2-k_{Fe,2D}^2) ,$$
$$\text{where } m_h^*=[m_{hh}^{*\,3/2}+m_{lh}^{*\,3/2}]^{2/3} . \quad (2)$$

m_{hh}^* and m_{lh}^* are, respectively, the heavy-hole and light-hole effective masses. In the second case, the current is off-resonant and, as in an Esaki diode, one expects a shoulder in the current corresponding to the complete overlap of the hole distribution at

$$eV_{1\text{-}3D}=\frac{\hbar^2k_{Fh}^2}{2m_h^*}(=\varepsilon_{Fh}) . \quad (3)$$

Because the values of $V_{1\text{-}2D}$ and $V_{1\text{-}3D}$ are close, and also because the features they represent in the current are not sharply defined, our experiment cannot clearly distinguish between the off-resonant and the resonant current at V_f. A second shoulder in the off-resonant current [Fig. 3(a), case δ] is expected at

$$eV_{2\text{-}3D}=\frac{\hbar^2k_{Fe,3D}^2}{2m_e^*}(=\varepsilon_{Fe,3D}) , \quad (4)$$

where m_e^* is the electron effective mass. This shoulder is not detected because at this point the resonant current is near its maximum [Fig. 3(b)]. After $V_{2\text{-}3D}$, the off-resonant current decreases and ideally vanishes when eV_b reaches ($\varepsilon_{Fh}+\varepsilon_{Fe,3D}$). The $N_{2D}(V_b)$ function has a maximum at

$$eV_{2\text{-}2D}=\frac{\hbar^2k_{Fe,2D}^2}{2m_e^*}(=\varepsilon_{Fe,2D}) \quad (5)$$

when the 2D electron distribution overlaps a maximum of hole states [Fig. 3(a), case γ] and then linearly decreases to zero as the overlap diminishes. However, caution is required in assigning the maximum in $N_{2D}(V_b)$ to the main peak voltage position V_p. This is because the width of the negative differential resistance region is narrower than that expected from the model. For this reason, the peak current has rather been ascribed to the disappearance of all the conducting channels between 2D electrons and 3D holes; that is to say when the ground state ceases to be resonant. Potential profile calculations under bias show that, at this point, the resonant level enters the GaSb band gap (a breakdown due to energy conservation) before going below the CB edge in the InAs emitter (an in-plane momentum conservation breakdown). Our description verifies, in accordance with Ref. 4, that superior peak current densities are obtained when tunneling occurs through 2D states.

Good agreement between the I-V curves and the model is obtained by applying a resistance correction of $R_c=R_c^{300\,K}+R_c^{\Delta T}=13.5\ \Omega$ to the experimental data at 4.2 K. This value was obtained by comparing the experimental peak position with the calculated voltage $V_p\simeq 160$ mV required to align the GaSb VB edge and the resonant level. With this value of R_c, the corrected voltage position of the low bias feature is 53 mV. This result is predicted from our model since the hole Fermi energy estimated from the doping density gives $V_{1\text{-}3D}=54$ mV [Fig. 3(b)]. The voltage position of the feature was determined by means of a second derivative technique (the inset of Fig. 2).

Hydrostatic pressure influences the I-V characteristics by changing the energy gap in the different material layers and also by increasing the electron and light-hole effective masses. The InAs band gap has a 10.0-meV/kbar pressure coefficient,[2] while the VB offset between GaSb and InAs increases by 3.0 meV/kbar.[12,13] Thus the energy difference (Δ) between the GaSb VB edge and the InAs CB edge across the GaSb/AlSb/InAs heterojunction decreases such that $d\Delta/dP\simeq -7.0$ meV/kbar. As a consequence, the Fermi energy of electrons in the well decreases and, similar to $V_{2\text{-}2D}$ [Eq. (5)], the peak position goes to lower biases. A quantitative estimate of the energy shift of the ground state can be made if the three following corrections are included in the previous simple picture (Fig. 1). First, the shifting of the

InAs CB edge with respect to the Fermi level is not uniform: it becomes smaller in the flat-band region of the InAs electrode, where $\varepsilon_{Fe,3D}$ decreases by 2.9 meV/kbar due to the 2.1%-kbar^{-1} InAs CB effective-mass pressure coefficient. Second, the energy shift of the resonant state is modulated by changes in the confining potential subsequent to charge removal from the well.[14] Third, the calculation of the confining energy of the ground state must account for the effective-mass pressure dependence. One experimentally observes a linear decrease of the peak position at a rate of $dV_p/dP \simeq -5.8$ mV/kbar. The calculated pressure dependence of the ground state is found to be 3.3 meV/kbar, from which a theoretical $dV_p/dP \simeq -6.6$ mV/kbar is obtained, considering an equal voltage drop from either electrode to the center of the well. The pressure dependence of V_f is related to the variation of k_{Fh}. E_{Fh} close to the barrier can actually be decreased indirectly by a pressure-induced charge removal from the well, and because of the requirement of electric-field continuity across the GaSb/AlSb/InAs region (Fig. 1). The voltage position of the feature decreases at a rate of $dV_f/dP \simeq -3.5$ mV/kbar whereas the change in E_{Fh} close to the barrier would induce a bias variation of $dV_f/dP \simeq -1.0$ mV/kbar.

Magnetic fields applied parallel to the current result in a linear decrease in both V_p (4.34 mV/T) and V_f (1.82 mV/T). At higher pressures both rates diminish, remaining in the same ratio of about 2.4. The shift of the peak to lower biases arises from a $\frac{1}{2}[\hbar\omega_c^h + \hbar\omega_c^e]$ energy decrease of the 2D-electron–3D-hole overlap ($\hbar\omega_c$ is the cyclotron energy). The $\frac{1}{2}\hbar\omega_c^h$ reduction of the hole distribution energy width ε_{Fh} entails a similar decrease of the low bias feature position, in accordance with Eq. (3) for the off-resonant process, and to first approximation with Eq. (2) for the resonant process. No magneto-oscillations are observed because the large Fermi energy for holes, $\varepsilon_{Fh} > \hbar\omega_c^e$ prevents resolving the individual Landau levels in the InAs well.[15] Both hydrostatic pressure and magnetic fields parallel to the current reduce the electron-hole overlap. However, pressure alone changes the whole band structure and affects the transmission probability. Practically, the current diminishes with pressure as InAs CB states align with evanescent states further into the AlSb band gap.

When transverse magnetic fields are applied,[8] the peak position undergoes a strong shift to *lower* bias voltages and the peak current decreases. This is radically opposed to results on type-I double-barrier diodes, which exhibit a B^2-dependent *increase* of their resonant peak position.[16] In this configuration the magnetic field provides the tunneling carriers with an additional momentum, so that the 2D electron and hole dispersion curves move away with respect to each other in k space. Because of their opposite curvatures, maintaining resonance (i.e., at least one intersection point between them) requires less bias as B is increased. From the V_p dependence upon B, one verifies that in this system the current cutoff originates from a well-collector type-II tunneling process rather than an emitter-well type-I process. This last point emphasizes the determining role played by the collector states in tunneling problems that are not easily revealed in type-I resonant tunneling structures.

This study discusses the various features in the current-voltage characteristics of double-barrier interband tunnel structures in terms of resonant and off-resonant current contributions. This picture was reasonably confirmed by pressure and magnetic-field experiments. Furthermore, specific to p-i-n structures, the cutoff of the resonant current component is determined by either energy or momentum conservation depending on the structural parameters.

We acknowledge the CNRS and the NSF under Grant Nos. ECS-8922512 and INT-8815314, and also NATO, the EEC, and the Conseil Regional Midi Pyrénées for financial support. F.A. is grateful to CAPES Brazil and D.K.M. is grateful for an EEC grant.

*On leave from Institut National des Sciences Appliquées, 31077 Toulouse, France.

†Present address: Department of Electron Physics, National Chiao-Tung University, Hsinchu, Taiwan.

[1] G. J. Gualtieri *et al.*, J. Appl. Phys. **61**, 5337 (1987).

[2] *Landolt-Börnstein Tables,* edited by O. Madelung and M. Schulz, New Series, Group III, Vol. 22a (Springer-Verlag, Berlin, 1982).

[3] L. F. Luo *et al.*, Appl. Phys. Lett. **55**, 2023 (1989).

[4] D. A. Collins *et al.*, in *Resonant Tunneling in Semiconductors,* edited by L. L. Chang, E. E. Mendez, and C. Tejedor, Vol. 277 of *NATO Advanced Study Institute, Series B: Physics* (Plenum, New York, 1991).

[5] L. Yang *et al.*, J. Appl. Phys. **68**, 2997 (1990).

[6] J. R. Söderström *et al.*, Appl. Phys. Lett. **55**, 1094 (1989).

[7] K. F. Longenbach *et al.*, Appl. Phys. Lett. **57**, 1554 (1990).

[8] E. E. Mendez *et al.*, Phys. Rev. B **45**, 3910 (1992).

[9] S. M. Sze, *Physics of Semiconductor Devices* (Wiley, New York, 1981).

[10] A. G. Chynoweth *et al.*, Phys. Rev. **121**, 684 (1961).

[11] E. O. Kane, J. Appl. Phys. **32**, 83 (1961).

[12] L. M. Claessen *et al.*, Phys. Rev. Lett. **57**, 2556 (1986).

[13] J. Beerens *et al.*, Phys. Rev. B **36**, 4742 (1987).

[14] E. E. Mendez, Surf. Sci. **267**, 370 (1992).

[15] E. E. Mendez *et al.*, Phys. Rev. B **43**, 5196 (1991).

[16] See, for example, L. A. Cury *et al.*, Superlatt. Microstruct. **7**, 415 (1990).